Proceedings of IMECE2005
2005 ASME International Mechanical Engineering Congress and Exposition
November 5-11, 2005, Orlando, Florida USA

IMECE2005-80616

PNEUMATIC BRAKE ACTUATOR DESIGN AND MODELLING FOR THE PRECISION STOPPING CONTROL OF AUTOMATED BUS

Fanping Bu **Han-Shue Tan**
California PATH
Institute of Transportation Studies
University of California at Berkeley
1357 S. 46th Street
Richmond, CA 94804

ABSTRACT

Precision stopping is an important automated vehicle control function that is critical in applications such as precision bus docking, automated truck or bus fuelling, as well as automatic intersection or toll booth stopping. The initial applications of this technology are most likely to be applied to heavy-duty vehicles such as buses or trucks. Such applications require specific attention to brake control since the characteristics of a typical pneumatic brake system of a heavy vehicle is inherently nonlinear with large uncertainties. The feasibility of providing a smooth precision stopping brake control based on a conventional pneumatic brake system has not yet been demonstrated. As the first step toward the fine braking control of conventional pneumatic brake system, this paper describes the design of a pneumatic brake actuator based on the "off-the-shelf" components for the precision stopping control of an automated bus and details the modelling of each components. In order to facilitate controller design, the complex "component by component" model is reduced to a more tractable one which still preserves the basic nonlinear characteristics of the original system. Both physical explanation and experimental data are provided to justify the model reduction and validate the simplified model which is used for controller design in [1]

INTRODUCTION

Automated vehicle control has been studied for many years in areas such as automated highway system (AHS), vehicle stability control, and driver assistance. Some research results have been applied to support real-world driver assistance applications such as adaptive cruise control, roll-stability control and parking assistance. However, several good candidates for early adaptations of a "true" automation are applications on heavy-duty vehicles [2] such as automated bus rapid transits [3], automated truck/container yard operations, heavy-duty vehicle maintenance automation, as well as automatic operations for specialty vehicles such as automated snow removal [4]. Many such operations require the stopping system to automatically control the heavy-duty vehicle to stop smoothly and precisely in a consistent way equal to or greater than those from an experienced operator. Docking bus precisely, backing automated trucks and trailers onto a platform, fuelling automated trucks or buses, as well as stopping automatically at intersections or toll booths are some examples.

Controlling a vehicle to a complete stop is one of the longitudinal vehicle control functions. In particular, it is essential that a bus or a truck can apply a very fine brake control in order to stop at a designated location exactly. Most of the prior research on vehicle longitudinal controls focuses on the areas of high speed platooning [5], adaptive cruise control [6] and string stability [7]. The works related to vehicle stopping or fine brake control are limited to the Anti-lock Brake System (ABS) [8], vehicle stabil-

ity or passenger cars equipped with a hydraulic brake [9]. The design of a precision stopping controller for a heavy-duty vehicle has not been fully examined and deserves a closer investigation.

Furthermore, most buses and trucks today are equipped with pneumatic brake systems that use compressed air as the energy medium. From the control point of view, the pneumatic brake system has several characteristics that make the control design difficult. First, the compressibility of air introduces a large time delay, which limits system bandwidth. Second, the dynamics of the pneumatic brake system are highly nonlinear because of the nonlinear pressure/air flow relationship. Third, the pneumatic brake system, when coupled with heavy-duty vehicle longitudinal dynamics, has large uncertainties. Many factors contribute to these uncertainties: changing supply pressures due to brake release, increasing brake temperature due to frequent braking, brake wear, large load variation and changing road surface conditions due to rain or snow. Even with all those potential disadvantages, it is still desirable that the automatic brake control system uses the existing pneumatic brake as the primary means of stopping control either by tapping into the braking control commands or including an add-on actuator. Using the existing pneumatic brake system allows the automated vehicle to maintain all its manual braking capabilities. The ability to remain "dual use" is one of the common requirement preferences for the early automation deployment requirements. Relevant work on the pneumatic brake in literature focuses mainly in the areas of ABS [10] and fault diagnosis [11]. A comprehensive brake model was developed for diagnosis purpose in [11], however it was too complex for control design. In [12, 13], a simplified linear model with time delay is developed based on input/output relationship, and is used for high speed longitudinal control. Recent literatures that relate to the subject of pneumatic actuator controls (e.g. for robot motion control) [14] suggest that nonlinear model based control laws achieve superior performance over their linear counterparts. One of the key points to the success of the advanced nonlinear model based controller for the precision stopping control of heavy-duty vehicle is to establish an accurate yet tractable nonlinear model for the pneumatic brake system and associated vehicle longitudinal motion.

The application example presented in this paper is the "precision stopping" of a 40 foot CNG bus for the Bus Precision Docking public demonstrations at Washington, D.C. in 2003. These precision docking demonstrations consistently achieved 1 cm lateral and 15 cm longitudinal accuracies. Such high docking accuracies would allow fast loading and unloading of passengers similar to that of trains and greatly reduce the stress of manual docking in a high throughput Advance Bus Rapid Transit system [3]. Precision docking and stopping can also be a useful component for the concept of an Advanced Maintenance Station [15], where quick fuel fill-up, washing, and maintenance can be automatically performed at the end of each run. To enable automatic control of the pneumatic brake system and maintains

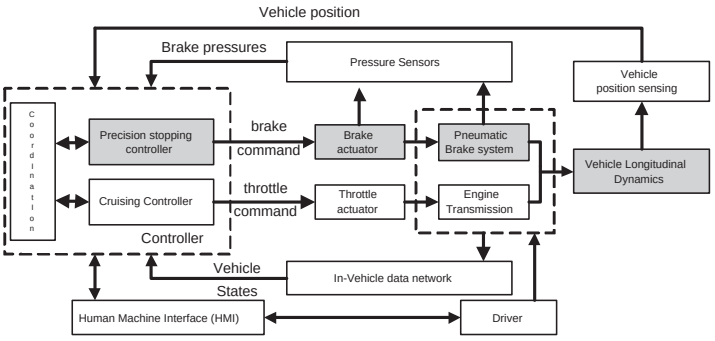

Figure 1. Schematics of a precision stopping system

the full integrity of the original air brake system, a general "brake by wire" system consisting of "off-the-shelf" pneumatic valves is proposed first. Secondly, the complex system model is obtained through modeling each individual component. In order to facilitate controller design, the complex "component by component" model is reduced to a more tractable one which still preserves the basic nonlinear characteristics of the original system. Finally, both physical explanation and experimental data are provided to justify the model reduction and validate the simplified model.

This paper is organized as follows: Section II introduces the precision stopping problem for heavy-duty vehicles and the design of pneumatic brake actuator; Section III describes the pneumatic brake system model and associated vehicle longitudinal motion; Section IV details the model reduction and validation; Section V concludes the paper.

Precision Stopping System, Pneumatic Brake Actuator Design and Automated Bus Configuration

Fig. 1 shows a general schematics of a precision stopping system based on a pneumatic brake system. The whole system includes cruise speed control, precision stopping control, coordination control and human-machine interface (HMI). The Precision stopping controller synthesizes a deceleration trajectory and the brake control command according to the sensor information. Sensor information could be air pressures inside the pneumatic brake system, vehicle states (e.g. vehicle speed, gear position and engine speed) and vehicle position. Most vehicle states are available through in-vehicle data network (e.g. J1939 bus for heavy-duty vehicles). Vehicle position can be obtained from GPS, magnetic markers or transbounders buried underground, video cameras and/or vehicle speed integration.

Fig. 2 shows the pneumatic loop of a typical heavy-duty vehicle air brake system. When the driver presses the brake pedal, the treadle valve is opened and compressed air flows from air tank to the brake chambers. The brake chamber is a diaphragm actuator which converts the energy of air pressure to the mechan-

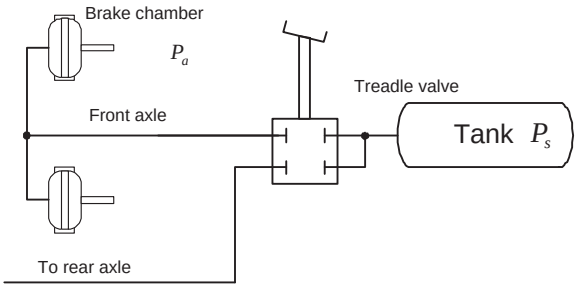

Figure 2. General schematics of pneumatic brake system

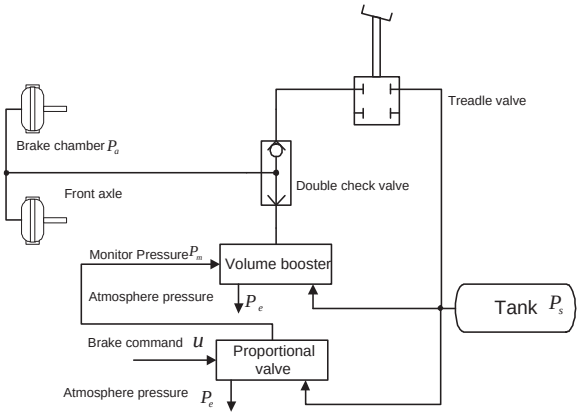

Figure 3. Schematic of front axle brake actuator (rear axle is similar)

ical force. Such mechanical force is transmitted to the brake pad through the push rod and brake cam. Brake force is generated by the friction between the brake pad and brake drum. Air is released to the atmosphere when the driver depresses the brake pedal. The compressor is turned on to recharge the air tank when the air tank pressure is below certain level due to air release.

A brake actuator receives brake control command and "actuates" the pneumatic brake system so that the desired brake force can be delivered to slow down the vehicle. The brake actuator can be designed in many ways, but it is desirable that it does not interfere with manual operation because of safety concerns. In [16], an electrical motor is added to control the brake pedal position. This method does not modify the original brake system, but it often introduces additional dynamics and nonlinearities such as brake pedal stiction. In [17], a "brake by wire" system (WABCO electronic braking system (EBS)) is used to replace the original air brake system. Inspired by the WABCO EBS design, this paper proposed a general "brake by wire" system consisting of "off-the-shelf" pneumatic valves, as shown in Fig 3. The design enables automatic control of the pneumatic brake system and maintains the full integrity of the original air brake system. A computer-controlled proportional pneumatic valve is installed between the air tank and brake chamber. In order to achieve a quick apply and release response, a volume booster is added into the loop to supply the air volume for a fast brake apply and release. Double check valve is used to ensure that the original air brake system will still be able to be operated by the brake pedal with the added hardware.

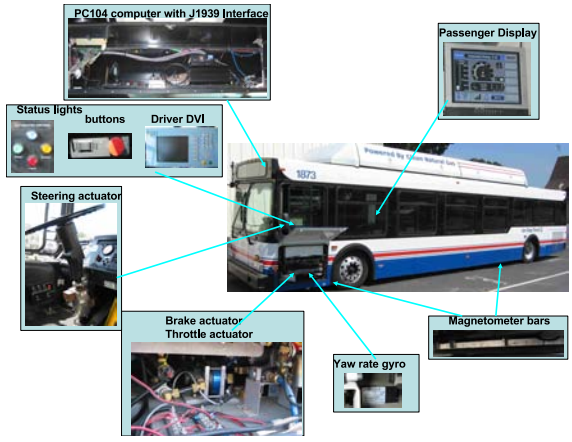

Figure 4. New Flyer CNG 40 footer bus configuration

Two New Flyer 40 footer CNG buses (c_1 and c_2) are retrofitted for the precision docking maneuver as shown in Fig 4. Magnetometer sensors are installed under the bus to detect magnets buried in the road with a meter spacing. The magnets provide both lateral and longitudinal positions. The throttle is modified so that it can be controlled through a computer. The original pneumatic brake system is retrofitted with the brake actuator design shown in Fig. 3. Pressure sensors are installed to measure internal pressures (monitor pressure P_m and chamber pressure P_a) of the brake actuator and the pneumatic brake system. The internal vehicle data network (J1939 bus) of the CNG bus is tapped to receive information on the engine and transmission states, such as vehicle speed, engine speed and gear position. The lowest speed that measures by the wheel speed sensor is about $0.6m/s$. Continuous longitudinal position is available by integrating the last magnet position and vehicle speed. Control and data collection program is running in a on-board PC104 computer under the QNX real-time operating system.

Pneumatic Brake System and Vehicle Longitudinal Motion Model

In this section, dynamic models for the brake actuator and the pneumatic brake system, as well as the vehicle longitudinal braking motion, will be developed.

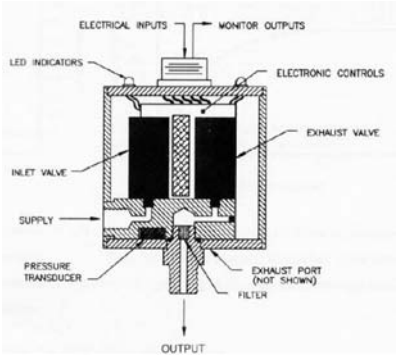

Figure 5. Schematic of a proportional pneumatic valve (Proportion-Air's QB1 valve)

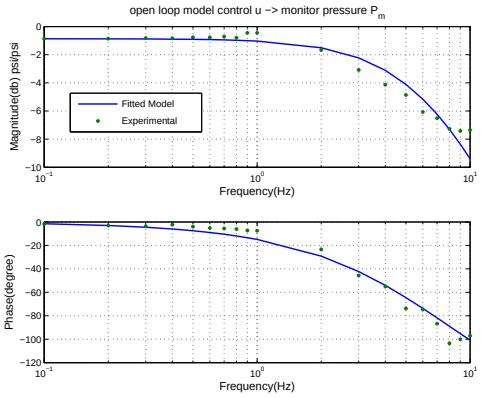

Figure 6. Frequency response of a proportional pneumatic valve (Proportion-Air's QB1 valve)

Modelling of brake actuator

As shown in Fig. 3 and Fig. 5, a proportional pneumatic valve is used in the brake actuator. Output pressure (monitor pressure P_m) is proportional to the electrical command input u. P_m is controlled by two solenoid valves inside the proportional valve. One such solenoid valve functions as the inlet valve, the other as the exhaust. P_m is measured by a pressure transducer internal to the proportional valve which provides a feedback signal to the electronic controls. Internal electronic control of the proportional valve serves as a closed pressure loop to maintain a linear relationship between the input command signal u and output pressure P_m. Because of the closed pressure loop and a very small air volume between the proportional valve's output port and the pilot input port of the volume booster, the dynamics of the proportional pneumatic valve can be approximated by a linear system. A frequency sweeping experiment is conducted to obtain frequency response from input command signal u_v to monitor pressure P_m for the Proportion-Air's QB1 valve in our experimental setup. The frequency response for this specific valve as shown in Fig. 6 can be fitted with a second order transfer function (1):

$$\frac{P_m(s)}{U_v(s)} = \frac{60.259}{s^2+17.465s+66.589} \tag{1}$$

Alone, especially when the brake is releasing, a typical small proportional pneumatic valve cannot provide enough air flow. Therefore, a volume booster is often mounted to improve response time. In our experimental setup, the Proportion-Air R series, as shown in Fig. 7, is used. The volume booster is an air-piloted, diaphragm-operated, self-venting regulator. Output pressure from the proportional valve is used as the pilot input pressure. The diaphragm is balanced by the input pilot pressure

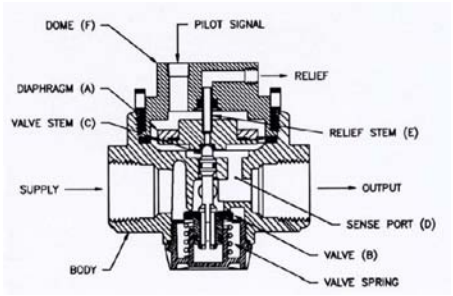

Figure 7. Schematics of a volume booster (Proportion-Air R series)

and the output pressure. Any difference between the pilot input pressure and the output pressure will move the diaphragm and open either the supply valve or exhaust valve so that the output pressure follows pilot input pressure. The air flow inside the volume booster can be described as, ideally, compressible gas passing through an orifice. As suggested in [18], we assume that

The air in the circuit behaves as an ideal gas
The density of the air int the circuit is uniform inside the pipe and brake chamber
The air in pneumatic circuit experiences isentropic processes

The air mass flow rate that passes through the volume booster can be expressed by:

$$\dot{m} = \begin{cases} C_s A_s(P_m, P_a) P_s \sqrt{\frac{2}{RT}} f(\frac{P_a}{P_s}) & r_s P_m \geq P_a(supply) \\ -C_e A_e(P_m, P_a) P_a \sqrt{\frac{2}{RT}} f(\frac{P_{air}}{P_a}) & r_s P_m < P_a(release) \end{cases} \tag{2}$$

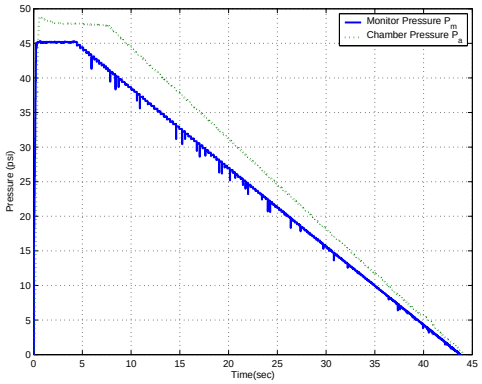

Figure 8. Pressure response of ramp valve input for our experimental setup

where $\dot{m}$ is the air mass flow rate that passes through the orifice, C_s and C_e are the orifice discharge coefficients, P_s is the air pressure inside the supply tank, P_a is the air pressure inside the brake chamber, P_{air} is the atmosphere pressure, $A_s(P_m, P_a)$ and $A_e(P_m, P_a)$ are the effective orifice areas which are functions of the pilot input pressure P_m and output brake chamber pressure P_a, R is the ideal gas constant, r_s is the effective area ratio between the two sides of the diaphragm, and T is the temperature. The piecewise continuous flow function $f(\alpha)$ is defined by:

$$f(\alpha) = \begin{cases} \sqrt{\frac{\gamma}{\gamma-1}(\alpha^{\frac{2}{\gamma}} - \alpha^{\frac{\gamma+1}{\gamma}})} & \alpha_c \le \alpha \le 1 \\ \sqrt{\frac{\gamma}{\gamma+1}(\frac{2}{\gamma+1})^{\frac{2}{\gamma-1}}} & 0 \le \alpha < \alpha_c \end{cases} \tag{3}$$

where α is the pressure ratio, γ is the specific heat ratio and α_c is the critical pressure ratio given by $\alpha_c = (\frac{2}{\gamma+1})^{\frac{\gamma}{\gamma-1}}$.

Fig. 8 shows the static response of the brake system in the experimental setup. The effective orifice areas are proportional to the pressure difference between P_m and P_a as shown in the following equation:

$$A_s(P_m, P_a) = k_s(r_s P_m - P_a) \quad A_e(P_m, P_a) = k_e(P_a - r_s P_m) \tag{4}$$

where k_s and k_e are constants that can be determined, for example, based on the relationship in Fig. 8.

Modelling of pneumatic brake

The brake chamber is a diaphragm-operated actuator which can be approximated by a single-acting pneumatic cylinder as shown in Fig. 9. $V_c(x_c)$ is the total air volume inside the brake chamber and the pipe between the volume booster and the brake chamber; and $V_c(x_c)$ is a function of brake chamber stroke x_c.

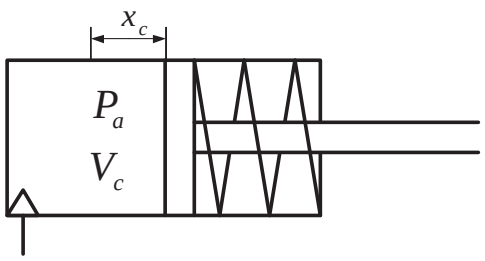

Figure 9. Brake Chamber

The pressure dynamics inside the brake chamber can be expressed by

$$\dot{P}_a V_c(x_c) + \gamma P_a \dot{V}_c(x_c) = \gamma \dot{m} R T \tag{5}$$

where the total volume $V_c(x_c) = V_d + A_c x_c$. V_d is the initial total dead volume before the brake is applied and A_c is the effective area of brake chamber. If we assume that the mass of the brake chamber push rod and brake chamber diaphragm can be neglected, the force balance on both side of the diaphragm can be described by:

$$k_r x_c = (P_a - P_{air})A_c - F_r \quad 0 \le x_c \le x_{cmax} \tag{6}$$

where k_r is the spring constant of the brake chamber return spring and F_r is the pre-load on the brake chamber return spring. The brake torque, T_b, acting on the wheel is proportional to the normal force acting on the brake pad

$$T_b = k_b((P_a - P_{air})A_c - F_r) \tag{7}$$

Modelling of vehicle motion during brake

A simple vehicle longitudinal braking dynamics can be described by [19]:

$$\begin{aligned} J_i \dot{\omega}_i &= R_i F_{bi}(\mu, \lambda_i, N_i) - T_{bi} - T_{tb} \\ M\ddot{x}_L &= -b\dot{x}_L - \textstyle\sum_{i=1}^{n} F_{bi}(\mu, \lambda_i, N_i) \end{aligned} \tag{8}$$

where i indicates the wheel number, ω_i is the wheel angular velocity, R_i is the rotational radius of ith tire, F_{bi} is the braking force generated by the ith tire, T_{bi} is the brake torque acting on the ith tire, T_{tb} is the equivalent braking torque generated by vehicle engine/transmission, x_L is the longitudinal position, M denotes the vehicle mass, b is the viscous damping coefficient, μ is the road surface friction coefficient, λ_i is the longitudinal slip of the ith wheel and N_i is the normal force at the ith wheel. The longitudinal slip λ_i is defined by $\lambda_i = \frac{\dot{x}_L - \omega_i R_i}{\dot{x}_L}$ when braking. The braking

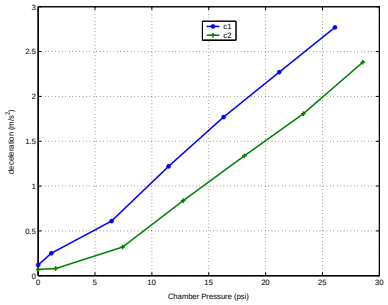

Figure 10. Deceleration vs brake chamber pressure of two different CNG buses (c1 and c2)

force $F_{bi}(\mu,\lambda_i,N_i)$ generated by ith tire is a highly nonlinear function of the road surface friction coefficient μ, tire longitudinal slip λ_i and normal force N_i.

Model reduction and validation

In this section, model reductions are made to facilitate controller design. Experimental data together with the physical explanations are used to justify the model reductions and to illustrate the accuracy of the resultant model.The proportional valve dynamics (1), the air flow equations (2-4), the chamber pressure dynamics equation (5), the brake torque generation equations (6-7), and the vehicle braking motion dynamics (8) represent accurate models of the pneumatic brake system and vehicle longitudinal motion during braking. They are rather complex for the controller design and many internal states are also difficult to measure (e.g. the brake chamber rod stroke x_c). Several steps of model reductions are made in this section to facilitate control design.

Model reduction

In the chamber pressure equation (5), the brake chamber volume $V_c(x_c)$ is comprised of the initial dead volume V_d and the variable volume $A_c x_c$ from the chamber rod motion. The variable volume $A_c x_c$ is small enough to be neglected so that the volume $V_c(x_c)$ can be assumed to be a constant due to its short brake chamber stroke. Then Eq. (5) is reduced to:

$$\dot{P}_a = \frac{\gamma RT}{V_c}\dot{m} \tag{9}$$

During the precision stopping, the vehicle braking is usually kept smooth to ensure the passengers' comfort. Therefore, the longitudinal slip λ_i is generally small during this stopping process. It is therefore reasonable to assume that the braking force is proportional to the brake chamber pressure P_a. For example, Fig. 10 shows experimental data between the brake chamber pressure and the bus deceleration for two different 40 foot CNG buses ($c1$ and $c2$). Although nonlinearities are dominant when chamber pressure is small, such a proportional assumption is good enough for the precision stopping control design when the brake pressure is, for the most part, sufficient large. Thus the brake torque generation equations (6-7) and the vehicle braking motion equation (8) can be simplified to:

$$M\ddot{x}_L = -F_b(P_a) - b\dot{x}_L\ , \quad F_b(P_a) = \zeta P_a + d \tag{10}$$

where ζ and d are unknown constants. ζ represents the combined effect of road surface conditions, brake conditions (wear, temperature) and vehicle load. And d represents the combined effect of engine/transmission brake and road friction.

Since the bandwidth of the proportional pneumatic valve is far larger than the required bandwidth of longitudinal control for precision stopping, the proportional valve dynamics are neglected and the monitor pressure P_m is defined as the control input u for the following controller design and implementation. The control input in implementation, the proportional valve command input u_v, is related to the control input P_m by a known static gain.

Define the state variables $x = [x_1, x_2, x_3]^T = [x_L, \dot{x}_L, P_a]^T$ and the unknown parameters as $\theta = [\theta_1, \theta_2, \theta_3] = [\frac{\zeta}{M}, \frac{b}{M}, \frac{d}{M}]$, the simplified system model, Eqs. (2-10), can be expressed in state-space form and linearly parametrized in terms of unknown parameters represented by θ as

$$\begin{aligned} \dot{x}_1 &= x_2 \\ \dot{x}_2 &= -\theta_1 x_3 - \theta_2 x_2 - \theta_3 \\ \dot{x}_3 &= \frac{\gamma RT}{V_c}\dot{m}(x_3, u) \end{aligned} \tag{11}$$

where $\dot{m}(x_3,u)$ is the nonlinear flow mapping inside the pneumatic brake system defined by Eqs. (2)-(5) and $u = P_m$.

Model Validation

Fig. 11- Fig. 13 show examples of comparisons between the experimental data from the demonstration setup (C2 bus) and the simulation results of the simplified pneumatic brake system Eq. (11) for both the monitor pressure P_m and chamber pressure P_a using various types of inputs for proportional valve (Fig. 11: sine wave; Fig. 12: stair step; Fig. 13: ramp input). The results show a good match between the simulation results of simplified model and the experimental data.

Conclusion

This paper presents a general "brake-by-wire" pneumatic brake actuator for the precision stopping control of automated

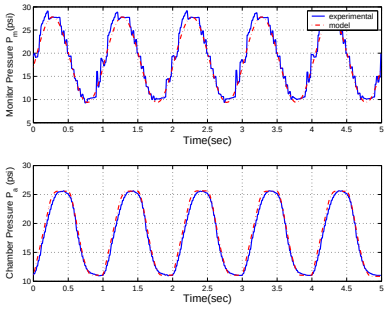

Figure 11. Simulation Results of Simplified Model vs Experimental Data 1: sine wave input

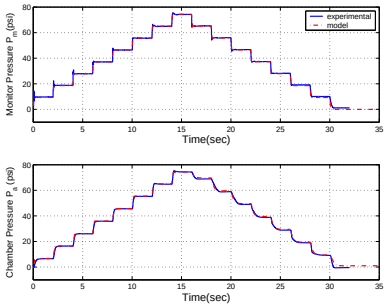

Figure 12. Simulation Results of Simplified Model vs Experimental Data 2: step input

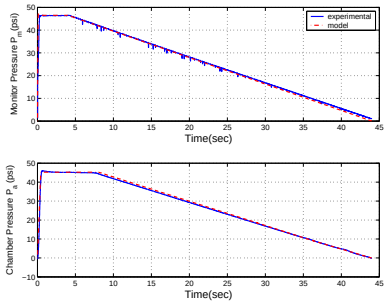

Figure 13. Simulation Results of Simplified Model vs Experimental Data 3: ramp input

bus. A detailed system model is setup by modelling each component. To facilitate controller design, model reduction is performed to achieve a more tractable one which still preserves the basic nonlinear characteristics of the original complex system model. Both physical explanation and experimental data are provided to justify the model reduction and validate the simplified model used for controller design in [1]. The presented brake actuator was implemented on two 40-foot CNG buses and was demonstrated at a precision docking demonstration in Washington DC during June 24-26, 2003. The successful 3-day public demonstration showcased the smooth stopping performance with consistent 15cm stopping accuracy under different operational conditions without a single failure.

ACKNOWLEDGMENT

This work was sponsored by the California PATH Program of the University of California, in cooperation with the State of California Business, Transportation and Housing Agency, Department of Transportation. The contents of this paper reflect the views of the authors, who are responsible for the facts and accuracy of the data presented herein. The contents do not necessarily reflect the official views or policies of the State of California. The authors wish to thank our colleagues, Ching-Yao Chan, Wei-Bin Zhang, David Nelson, Thang Lian and Susan Dickey for their generous supports and contributions in the study.

REFERENCES

[1] Bu, F., and Tan, H.-S., 2005. "Precision stopping control of automated bus with pneumatic brake system". In Proc. of IEEE/ASME International Conference on Advanced Intelligent Mechatronics (AIM), pp. 116–121.

[2] Bishop, R., 2000. "Intelligent vehicle applications worldwide". IEEE Intelligent Systems, **15** (1) .

[3] Donath, M., SHankwitz, C., Alexander, L., Gorjestani, A., Cheng, P., and Newstrom, B., 2003. Bus rapid transit lane assist technology systems. Tech. rep., University of Minnesota.

[4] Tan, H.-S., 2004. "An automated snowblower for highway winter operation". Intellimotion, **10** (4) , pp. 1–2.

[5] Rajamani, R., Choi, S. B., Law, B. K., Hedrick, J. K., Prohaska, R., and Kretz, P., 2000. "Design and experimental implementation of longitudinal control for a platoon of automated vehicles". Transactions of ASME, Journal of Dynamic Systems, Measurement, and Control, **122** (September) , pp. 470–476.

[6] Liang, C., and Peng, H., 1999. "Optimal adaptive cruise control with guaranteed string stability". Vehicle System Dynamics, **32** (4) , pp. 313–330.

[7] Swaroop, D., and Hedrick, J. K., 1996. "String stability of interconnected systems". IEEE Transactions on Automatic Control, **41** (3) , pp. 349–357.

[8] Hatipoglu, C., Hai, Y., and Ozguner, U., 2001. "Self-optimizing brake control design for commercial vehicles". In SAE Technical Paper, no. 2001-01-2731.

[9] Choi, S. B., and Devlin, P., 1995. "Throttle and brake combined control for intelligent vehicle highway systems". In SAE Technical Paper, no. 951897.

[10] Acarman, T., Ozguner, U., Hatipoglu, C., and Lgusky, A., 2000. "Pneumatic brake system modeling for systems analysis". In SAE Technical Paper, no. 2000-01-3414.

[11] Subramanian, S. C., Darbha, S., and Rajagopal, K., 2004. "Modeling the pneumatic subsystem of a s-cam air brake system". Transactions of ASME, Journal of Dynamic Systems, Measurement, and Control, **126** (1) , pp. 36–46.

[12] Yanakiev, D., and Kanellakopoulos, I., 2001. "Longitudinal control of automated chvs with significant acutator delays". IEEE Transactions on Vehicular Technology, **50** (5) , pp. 1289–1297.

[13] Lu, X., and Hedrick, J., 2003. "Longitudinal control design and experiment for heavy-duty trucks". In Proc. of 2003 American Control Conference, pp. 36–41.

[14] Bobrow, J., and McDonell, B., 1998. "Modeling, identification, and control of a pneumatically actuated, force controllable robot". IEEE Transactions on Robotics and Automation, **14** (5) , pp. 732–742.

[15] , 1999. Intelligent vehicle initiative needs assesment. Tech. Rep. FTA-TRI-11-99-33, Federal Transit Administraion.

[16] Alexander, L., and Donath, M., 2000. Differential gps based control of a heavy vehicle. Tech. Rep. 2000-05, University of Minnesota, Twin City.

[17] Dickey, S. R., and Lu, X. Y., 2003. "Control actuation of fully automated heavy-duty vehicles using sae j1939". In Proc. IEEE Intelligent Vehicles Symposium (IV2003), pp. 400–405.

[18] Bigras, P., and Khayati, K., 2002. "Nonlinear observer for pneumatic system with non negligible connection port restriction". In American Control Conference, pp. 3191–3195.

[19] Lee, K., Jeon, J., Hwang, D., and Kim, Y., 2003. "Performance evaluation of antilock brake controller for pneumatic brake system". In Proc. IEEE Industry Applications Conference, vol. 1, pp. 301–307.